LUCI in the sky: performance and lessons learned in the first two years of near-infrared multi-object spectroscopy at the LBT

Peter Buschkamp*[a], Walter Seifert [c], Kai Polsterer [b], Reiner Hofmann [a], Hans Gemperlein [a], Reinhard Lederer [a], Michael Lehmitz [d], Vianak Naranjo [d], Nancy Ageorges [e], Jaron Kurk [a], Frank Eisenhauer [a], Sebastian Rabien [a], Mathias Honsberg [a], Reinhard Genzel [a]

[a] Max-Planck Institut für extraterrestrische Physik, Postfach 1312, 85741 Garching, Germany;
[b] Astronomisches Institut Ruhr-Universität Bochum, Universitätsstr. 150, 44780 Bochum, Germany;
[c] Landessternwarte Heidelberg, Königstuhl 12, 69117 Heidelberg, Germany;
[d] Max-Planck Institut für Astronomie, Königstuhl 17, 69117 Heidelberg, Germany;
[e] Kayser-Threde GmbH, Perchtinger Str. 5, 81379 München, Germany

ABSTRACT

LUCI (former LUCIFER) is the full cryogenic near-infrared multi-object spectrograph and imager at the LBT. It presently allows for seeing limited imaging and multi-object spectroscopy at R~2000-4000 in a 4x4arcmin^2 FOV from 0.9 to 2.5 micron. We report on the instrument performance and the lessons learned during the first two years on sky from a technical and operational point of view. We present the upcoming detector upgrade to Hawaii-2 RG arrays and the operating modes to utilize the binocular mode, the LBT facility AO system for diffraction limited imaging as well as to use the wide-field AO correction afforded by the multi-laser GLAO System ARGOS in multi-object spectroscopy.

Keywords: NIR, imaging, spectrograph, MOS, multi-object spectroscopy, cryogenic, LBT, performance

1. INTRODUCTION AND OVERVIEW OF THE INSTRUMENT

LUCI (former LUCIFER, Seifert et al. 2003, [6]) is the full-cryogenic near-infrared camera and multi-object spectrograph at the Large Binocular Telescope on Mt. Graham, Arizona. It has been developed by the Landessternwarte Heidelberg, the Max-Planck Institute for Extraterrestrial Physics, the Max-Planck Institute for Astronomy and the Astronomical Institute of the University of Bochum. Each eye, i.e. primary mirror, of the LBT has its own LUCI. Both instruments are identical in functionality and available observation modes. LUCI-1 had first light on 6 September 2008 and is in regular science operations since fall 2009, with the MOS unit for multi-object spectroscopy being offered for science users since beginning of 2010 Commissioning and performance results were presented in Ageorges et al. (2010) and Seifert et al. (2010) [1],[7]. LUCI-2 is currently undergoing final lab testing and is scheduled for installation in late 2012 with commissioning following in early 2013. Once both instruments are installed, they can operate independently or in sync in binocular mode.

LUCI currently features seeing limited imaging at pixel scales of 0.12" and 0.25"/pixel and spectroscopy at R~2000-4000 from 0.9 to 2.5 micron in a 4x4 arcmin^2 FOV. The instrument has a built-in upgrade path for utilizing the facility adaptive-optics system of the LBT. The necessary upgrades and components are currently manufactured, tested, and integrated and will enable diffraction-limited imaging over a 30x30 arcsec^2 FOV as well as high resolution spectroscopy. Commissioning of the diffraction limited observing modes using natural guide stars is presently scheduled for the first half of 2013. Adaptive optics using the laser guide star will be commissioned after the installation of the ARGOS laser guide star system, i.e. in later 2013. Once both LUCI instruments are installed the maximum angular separation of the two instrument's FOVs on sky will be ~40arcsec. This is due to the binocular mount design of the LBT where the placement of the FOVs is limited by the working range of the active optics system.

*Correspondence should be send to: Peter Buschkamp; email: buschkamp@mpe.mpg.de; phone +49 89 30000 3295

Imaging in LUCI is done with three different cameras having different focal lengths. The two cameras for seeing limited observations are refractive systems, the diffraction limited camera follows a Cassegrain design. The 'N3.75' camera images the FOV on the full 2k×2k pixel Hawaii-2 detector, which results in a resolution of 0.12 arcsec/pixel (0.24″ Nyquist sampled resolution). The 'N1.8' camera images the FOV on a quarter of the detector centered on the detector (i.e. 0.24arcsec/pixel= 0.48″ resolution). The latter camera looks beyond the instrument FOV, partly imaging the (dark) 'inside of the instrument'. This is on purpose as it is used for spectroscopic applications, where the full spectral NIR band (J, H or K) needs to be recorded and the angular dispersion in turn extends the spectrum beyond the 4′×4′ field (assuming a slit centered in the FOV and the grating-tilt adjusted such that the band's central wavelength is at the center of the detector).

In spectroscopic mode, the user can chose between three gratings depending on the desired resolution and wavelength coverage. The grating replaces the imaging mirror in this mode. In summary, a multi purpose grating covers z, J, H and K-band spectroscopy at a resolution ~7000 for a 2-pixel (Nyquist sampled) slit. Depending on the camera, full-band spectra extend partly beyond the detector area. The two other gratings serve a special purpose: One acts as an H+K grating at a resolution of ~2000 for seeing limited or as an H *or* K grating for AO assisted observations at R~4000 (again 2-pixel slit). The third one is a single purpose grating: it delivers a resolution of ~4000 at a high efficiency in Ks for a seeing limited 0.5″ slit. Spectroscopy can either be done in longslit or multi-object-slitmask (MOS) mode. For longslit observations, the unique MOS unit provides the instrument with MOS masks that contain only one longslit. In MOS mode, 23 custom made exchangeable multi-slit masks can be stored and used in the instrument. The masks are laser cut and are exchanged using auxiliary cryostats while preserving cryogenic conditions. These auxiliary cryostats temporarily attach to the main cryostat during the mask cabinet exchange.

This paper is organized as follows: In chapter 2, we present the current hardware status and changes introduced over the first years of operation. In chapter 3, we discuss the control software. The system performance on sky is presented in chapter 4. To close, we present in chapter 5 the upcoming upgrades to the instrument and briefly discuss the upcoming observation possibilities afforded by the binocular mode, the LBT facility AO system, and the ground layer laser AO system ARGOS.

2. HARDWARE STATUS AND CHANGES

In the following, we present the current hardware status and changes introduced over the first years of operation. Except for the detector, which was lost due to an accident and had to be replaced, the instrument hardware has not seen major changes or revisions. We have replaced a few moving parts to improve the reliability of the unit, those changes could be implemented during the scheduled maintenance periods during the annual summer-shutdown of the observatory.

2.1 Detector

The original detector, which had been in use in LUCI-1 during the first two years of operation, has recently been exchanged: on 12 October 2011 the original Hawaii-2 array of LUCI-1 was lost due to human error and technical malfunctions while in cryogenic condition. During the cool-down phase, the detector was exposed to a thermal gradient of > 4 Kelvin/minute. The silicon layer separated from the substrate and shattered, destroying the detector. This incident caused a five months down-time of the instrument for repair. As the debris of the detector was dispersed inside the instrument during the unavoidable rotation and tilting while transporting it back to the mountain lab, the instrument had to be disassembled completely for the clean-up procedure. Debris was even found inside the bearings of several moving components, e.g. the grating and filter wheel, rendering these components inoperable.

To minimize the down-time, it was decided to use the LUCI-2 detector in LUCI-1 as an interim solution. Table 1 shows a comparison of the old and the new interim detector.

Table 1. Characteristics of the LUCI-1 detector.

	old detector	**new detector** (interim, taken from LUCI-2)
Pixelsize	18μm x 18μm	
Number of pixels	2048 x 2048	
Fullwell	~235000 e⁻	~257000e⁻
Linearity within 5%	up to 90% full well	up to 80% full well
QE in observing bands	z: 0.25; J:0.33; H:0.74; K:0.73	z: 0.37; J:0.48; H:0.55; K:0.57
Readout modes	Double-Correlated Reads (DCR) Multiple-Endpoint Reads (MER, 10 samples)	
Gain (in DCR)	4.08e⁻/ADU	4.5 e⁻/ADU
Read noise	11.9(DCR); 5.7(MER) e⁻	12.6 (DCR), 7.6(MER) e⁻
Dark current (in DCR)	0.06 e⁻/s/pixel	0.04 e⁻/s/pixel

The interim detector has a higher quantum efficiency (QE) in J-band but a significantly lower QE in H- and K-band. Gain, read-out noise, and dark current are similar. The cosmetics are comparable to the original detector, however, it shows some persisting electronic noise pattern especially near the boarders of the readout channels. We have found that by using a slightly modified readout scheme in double correlated readout we can remove the pattern for all practical purposes. For a double-correlated readout, we now read the array two times before and after the integration, throwing away the first pair and only correlating the second pair.

As a result, LUCI-2 lacked a detector, and it was decided to upgrade both instruments to the newest 'Hawaii-2 RG' 2kx2k detector array. LUCI-2 will feature the new detector when it is shipped to LBT later this year, LUCI-1 will be upgraded on site thereafter. The detectors require a different back-end electronics and detector mount stage as discussed below.

2.2 MOS Unit

The MOS unit for storing and handling the spectroscopic long- and multi-slit masks is the most complex unit inside LUCI with its cryo-mechanical structure and the numerous diverse motions and their interplay it provides. A detailed description of the MOS unit's functionality and structure can be found in Buschkamp et al. 2010 [2]. We here give an overview of its performance and present some of the changes we have introduced in the last two years.

Over 4500 mask exchanges have been run so far during commissioning, test and science nights. The typical failure rate on the level of individual mechanical movements is of the order 0.1%, but since a mask exchange (the observation-relevant movement-collection) consists of several movements, the failure rate on the operations level in- creases to overall about 1%.

Most of these occasionally occurring errors so far could be corrected using the built-in software based recovery functions. In these cases, the science observation preparation (acquisition time) typically increased by several minutes or single science frames were lost, but observations could still be carried on during the night.

We have encountered a stop of science observations several times, requiring a manual debug of the MOS unit, typically resulting in a 30–180min loss in observing time. Very few times, however, error recovery required interventions on the hardware engineering level, i.e. recovering the unit or swapping electronics components during daytime or even warming up the instrument. In those few cases, science nights were lost or observations could only continue in LUCI imaging-only mode or with other instruments (i.e., MOS repair during daytime) or the instrument was unavailable for 2-3 weeks

in case a warm-cold cycle of the instrument was needed for a repair. Major failures subsequently lead to hardware upgrades during the annually scheduled maintenance runs. The upgrades enhanced the hardware as well as the automatic correction and auto-debug capabilities and led to an increase in reliability of the unit by a factor ~2.

The following two examples were the most frequently encountered errors:

Mask grabber malfunction: The mask grabber drives utilizes a ball screw that is comparably small and thus rather sensitive for abrasion and accumulation of dust particles. We have meanwhile replaced the drive screw in a maintenance run. A permanent fix is not yet identified as the available space in the grabber head is rather tight. An approaching malfunction can be estimated by monitoring the number of steps the grabber needs to open or close. We have implemented an auto correction based on back-and-forth motions, however, if the unit gets stuck when too much dust has accumulated due to abrasion, the ballscrew needs to be replaced, requiring a warm-up of the cryostat.

Limit and position-switch malfunction: Single limit and position-sensing switches have shown sporadic errors. Limit switches are used to calibrate motions, they cannot be simply ignored. A recovery always requires a trained person to debug the unit manually on the engineering level. Position switches can be retried by repetitive motions. We have found that the deployed spring-switches sometimes change their mechanical behavior or responsivity significantly in cryogenic conditions. The means and direction of actuation were changed subsequently for some switches which significantly improved their reliability.

As a consequence of the observed behavior of the spring-switches, we have altered the design of position sensing-switches used in the complex mask-retainer in LUCI-2. Each of the arms (whose function it is to free an individual mask for manipulation by the mask robot) now carries a small Nd-magnet, that actuates a reed-switch to indicate the open-state when the arm is retracted. This design change has also decreased the force against which an arm has to be retracted. Albeit small, the force of the switch's spring-lever has been observed to be sufficient to prohibit full retraction of an arm in cryogenic conditions several times.
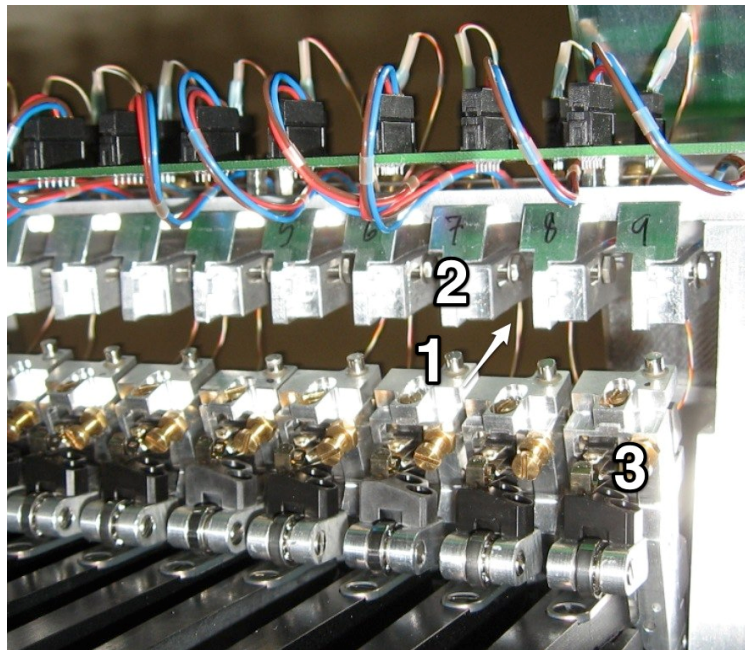
Figure 1: Revised retainer arm open-state switches with the magnets (1) and reed switches (2) marked. The arrow next to them points in the direction of the retracting motion. For mask sensing, we still use spring loaded switches (3). See [2] for a detailed description of the retainer.

Generally, we have found, that the wear of the cryogenic gears and ball screws is slightly higher than expected. For the parts that were coated with the dry-lubricant DICRONITE we have not seen a substantial improvement in reliability over non-coated parts.

The cabinet transfer scheme for exchanging used and new masks in the instrument cryostat uses two dedicated auxiliary cryostats. This procedure has shown to be comparably labor-intensive. Currently there exists no alternative method to exchange used and new masks, however, we investigate alternatives, especially those that would feature an exchange mechanism that can be manipulated from outside or simply relies on manual operation using vacuum feed-throughs.

Cabinet transfer failure: On 6 March 2012, a cabinet could not be transferred from the LUCIFER cryostat to the attached auxiliary cryostat. The draw bar of the cabinet had warped and hit the bearing of the cabinet drive inside the auxiliary cryostat, preventing it from further moving on into the auxiliary cryostat. As the cabinet could be moved back into LUCIFER but not be extracted, the LUCIFER cryostat had to be warmed up to remove the cabinet and restore mask exchange functionality. This rendered the system inoperable for 3 weeks. Meanwhile all cabinets have been outfitted with a stronger draw bars.

2.3 Camera wheel

The camera wheel holds the three different cameras (the N1.8 and N3.75 camera used for seeing-limited operation and the N30 camera for diffraction limited observations), and rotates them into the beam in front of the detector. The camera wheel has a circumferential gear and is actuated by a stepper motor that attaches to it with a cogwheel. The travel range of the wheel is 270 degrees and two limit switches stop the motion in either direction near the mechanical motion limits of the wheel. Camera position sensing is done via spring switches, which we actuate with notches on the camera wheel.

We have encountered erratic readings of the camera position switch in several cases that led to an incorrect positioning of the camera with respect to the optical beam. It was found, that the exact shape of the notches has a strong influence on the switching-behavior of the deployed switches, which -in cryogenic conditions- could cause the switch *not* to switch although it was actuated. This is similar to the behavior we have encountered with some of the MOS's state- and positioning switches as discussed above.

In a now updated version we have optimized the shape of the notches leading to a greatly improved reliability of the switches.

2.4 Flexure compensation

We compensate the flexure resulting from rotating and tilting the instrument by moving the last mirror in the optical train of LUCI, which is placed before the instrument's internal pupil. The motion of the corresponding folding mirror is carried out according to a lookup table. Presently, there is no active flexure compensation using e.g. an optical alignment laser or strain gauges for feedback.

Calibration of the motion is done by moving against a reference surface, which in the first hardware version was simply a stainless steel part in the mirror mount. After several months of operation, severe degradation was observed in the performance of the flexure compensation. The hysteresis in the motion increased to a level where reliable operation was no longer possible. It was found that the motion had damaged the reference surface causing grooves and dents.

In an updated version we now use ceramic blocks as a reference. This has significantly improved the reliability and performance and so far the flexure compensation has shown no performance degradation over time. An update to a active flexure compensation is currently being investigated (see below).

3. CONTROL SOFTWARE AND USER GUIS

The LUCI control software was designed and implemented as a multi-tier distributed system. Multi-tier client-server and service-oriented architectures (SOAs) are very effective design patterns. Individual services provide an easy way to separate tasks, to increase abstraction and reusability, to allow autonomous execution, and to encapsulate complex algorithms as well as data structures. A typical example of SOAs are modern UNIX-like operation systems that gain stability with independently start- and stoppable daemons.

The chosen multi-tier architecture allows to hide complexity within a tier and to provide simple and powerful functions to services of a higher tier. This concept was applied in the development of the high level service architecture. A distributed system was chosen to increase scalability and interoperability of the software. The individual services are grouped into four tiers: the System-Tier, the Control-Tier, the Instrument-Tier, and the Operation-Tier.

The System-Tier contains all frameworks to run and control a distributed system, to allow central configuration management, persistent storage of data in a database and message generation in order to track the state of the system. Beside the basic services for messages and configuration management, the System-Tier includes frameworks to implement internationalisation, resource bundling, and tools to improve source documentation and message database-mining.

The Control-Tier reflects the hardware-software interaction. An RS232 communication framework is used in each of the hardware controlling services. These services are grouped in environment supervising services and into services that communicate with the motion control electronics. This tier contains a service that tracks the instrument state as a central logging mechanism. All hardware interacting services report to this logging service. The detector readout software and the interface to the telescope are also a part of this tier.

The Instrument-Tier is responsible for the motion logics needed to set up the optical and mechanical components of the instrument. It uses the hardware communication provided by the Control-Tier. As the central component, the sequence execution framework provides easy composing and execution of complex motion sequences. All motions within LUCI are modeled as finite-state transition networks. This approach has proven to be very versatile and reliable especially due to the applied scheme of defined pre- and post-conditions for every motion sequence and is fundamental to an efficient usage of the LUCI instrument.

At the topmost level, the Operation-Tier contains all services needed to operate the instrument. This includes the coordination of the services of the Instrument-Tier and the supervision of the instrument environment as well as the interaction with the external software packages of the readout and telescope control software. The GUIs used to grant engineering access as well as an observations scripting mechanism are another part of this tier. Some services of this tier are still missing or are in a preliminary state. For a binocular use of both instruments, these services are mandatory and are currently being finalized.

The first years of operations have shown that the chosen approach of distributed services combined with the capability to automatically restart broken or stopped services on demand, grants an enormous robustness to the control software. Up to now, no observation was interrupted or hampered by a failing service. In case of errors, services have been isolated, tested and replaced without affecting the remaining system. The complexity to maintain the whole system was reduced to the complexity to maintain a single service. A clear interface definition of each service allows to replace its implementation independently. We have extended the logging capabilities to allow for more in-depth logging of the server-instrument communications as well as the exact instrument state. This has enabled us to trace down errors much more efficiently, e.g. it helped tracing a firmware error in the motion controller hardware. New web-based tools have been developed to allow for an efficient search the database entries used for logging. Today, we would directly implement such a database logging in any communication with external devices and external software packages. This would have significantly minimized the time spent to debug errors during operation. Some preliminary software elements which have been developed for testing purpose or to expand functionality are still in use to date. These 'workarounds' now require some extra efforts on the side of software development to support the upcoming binocular observations and the use of adaptive optics. E.g., the creation of the fits-header was spread over all participating services to have more flexibility in adding additional content. In a two-instrument situation this now needs to be taken away from the individual services and header-creation will be centralized in the in the readout service.

For testing purpose, we have created a virtual instrument in an early phase of the control software development. This simulator often enabled us to test new motion sequences prior to run them on the real hardware and therefore to detect

bugs in the software. This simulator was presented in Polsterer et al 2006 [4]. To date it still serves an important role in debugging and testing and is used to train technical personnel on the engineering level. The 3D model view of the virtual instrument shown in figure 2 can be connected to the real hardware to visualize the current hardware state which facilitates debugging.
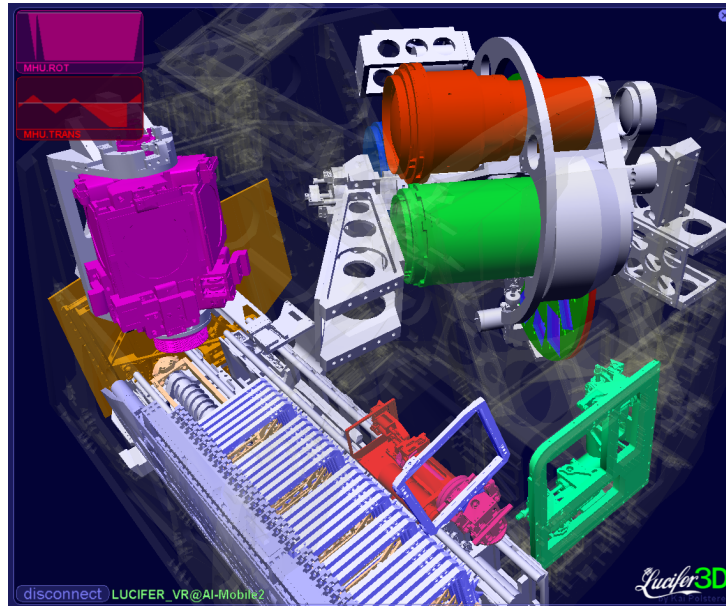
Figure 2: LUCI 3D , the visual representation of the virtual instrument using the actual CAD model of LUCI. All movements are done in real time, changes on the engineering GUI are reflected like in the real instrument. the figure shows (clockwise from top) the camera wheel with the cameras, the focal plane unit (lower right), the MOS unit (bottom) and the grating wheel unit (left). Additional information, e.g., plots of stepper motor motion progress can be displayed as an overlay (upper left corner)

4. SYSTEM PERFORMANCE AND OPERATIONS

In the following, we show the system performance on sky and discuss the current operation modes.

4.1 System efficiency in spectroscopic mode

The system efficiency in spectroscopic observing mode was measured on sky using standard stars under typical observing conditions for the LBT site. We have used a 2″ slit so that slit losses are not affecting our measurement. The system efficiency measurements for grating 2 in H and K band are presented in figure 3. We show the total efficiency, i.e. the measurement includes the telescope. As a detailed transmission curve for the telescope is not available its effect cannot be accounted for. We have corrected for the atmospheric transmission. Measurements for z, J, H, and K band separately using the dedicated z, J, H, K-grating with the new detector are pending.

The calculated efficiency is shown in black with its axis on the left given in percent. We also plot the atmospheric sky emission in orange (axis on the right) normalized to the intensity of brightest OH line within the respective NIR band. This is to guide the eye when evaluating the efficiency in 'usable' wavelength intervals in the near-IR, i.e. between the OH molecular series. The slight mismatch between the calculated and observed atmosphere introduces some residuals

which make these variations by the filter transmission curve less visible. The general shape of the efficiency is dominated by the grating and the detector efficiency curve.
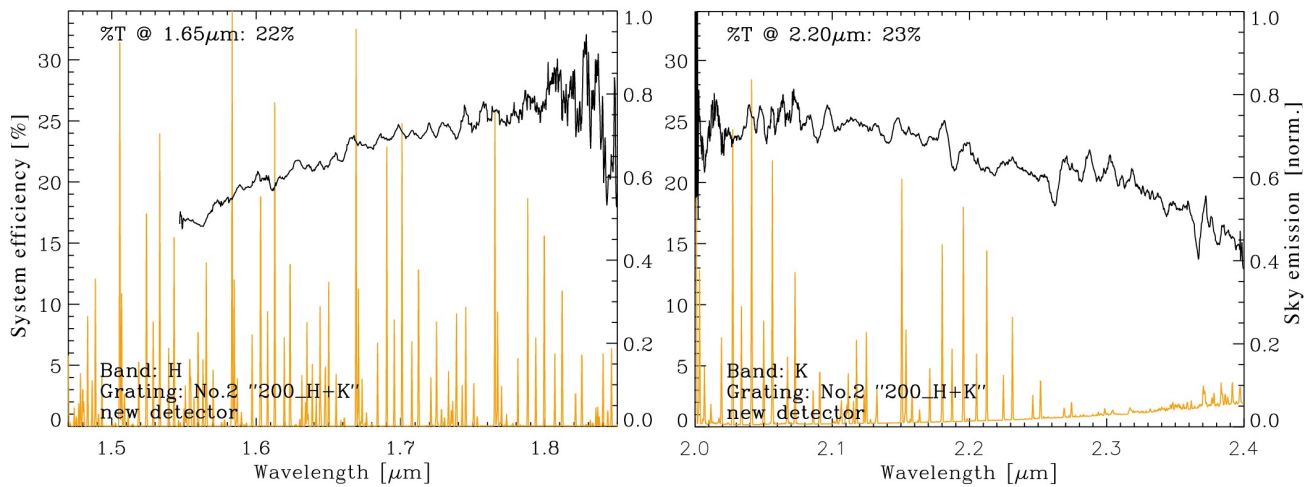
Figure 3: System efficiency in H-band (left) and K-band(right) using the H+K grating. The efficiency curve is shown in black. The sky emission from OH molecules and the thermal background that rises in the far K band are plotted for reference.

The maximum efficiency of ~25% and the shape of the efficiency curve are in very good agreement with the theoretical efficiency calculated from the performance values of the various components. It is comparable to other NIR spectrometer featuring a similar detector array. We note that the system efficiency will rise significantly once the new Hawaii-2 RG detectors are installed. While the quantum efficiency of the current detector in H and K-band is ~55%, the new array has been measured to achieve 85% quantum efficiency at 1µm and 82% QE at 2µm. Given these values we have calculate a system efficiency of up to 40% using the new 'RG' detectors, significantly boosting efficiency on sky.

4.2 Overall performance and operations

To date, the system efficiency is comparable to or exceeds other NIR (multi-object) spectrometer (where published values or performance reports are available), and will be even more so once the new detector will be installed towards the beginning of next year. This applies both to imaging and spectroscopy. The two camera design means that there is no tradeoff between imaging and spectroscopy and the different gratings optimize efficiency and offer useful resolutions in seeing and -in the future- diffraction limited observations. The reliability of the unit is good with occasional errors, which, however, after various upgrades, have not lead to major time loss in recent times as compared to the first months on sky. The versatility afforded by the diverse operation modes makes LUCI a very competitive instrument, especially with the upcoming adaptive optics assisted observation modes.

LUCI relies on a complex interplay of various units. The compact design and design-changes late in the project (e.g., the exchange of the integral-field unit with the MOS unit) have led to some complications that caused some designs, especially of the MOS unit, to be rather complex. Various hardware simplifications were introduced in the last years, however, some designs cannot be changed with the instrument now completed. We have addressed some more basic issues found with LUCI 1 (e.g., the mask retainer, see above) in LUCI-2. Small errors in some of the LUCI sub-units, especially the MOS, could still potentially cause downtime, their replacement and/or more sophisticated auto-correction software sequences are being investigated. Flexure compensation is still an active area of work. The image movement using the N1.80 spectroscopic camera is around 5 pixels when flexure is uncompensated. Due to hysteresis effects of the passive flexure compensation solution, up to one pixel image motion is still remaining when flexure is compensated. A design change is being investigated (see below). The present design of the grating tilt units using open coil motors allows for a very precise alignment of the central wavelength by a closed loop operation, however, the stabilization is loosing accuracy for zenith distances <10 degrees due to the large forces introduced by the fast turning instrument rotator. This leads to some limitations in usage.

On-site operations have greatly improved over the last two years, however, a significant fraction of lost observing time can still be attributed to observational errors. The complexity of the instrument can be demanding for new observers and a careful preparation of observations and observation-scripts is key to successful observations. A more user friendly GUI is presently being developed taking into account feedback from the science users. It will help to increase observing efficiency especially if on-the-fly changes to the instrument and telescope configuration are needed.

The laser-cut, i.e. static, user provided MOS masks have proven to be very reliable. Mask exchange times of $<\sim 5$ minutes are only a small fraction of the overall acquisition and setup time prior to an observation block. Currently the turnaround time for new masks from design to availability in the instrument is about one month.

5. UPCOMING UPGRADES

To close, we present the upgrades to the instrument happening in the near future and discuss the upcoming observation possibilities afforded by the LBT facility AO system and the ground layer laser AO system ARGOS.

5.1 Detector upgrade to Hawaii-2 RG

The new Hawaii-2 RG detectors in LUCI 1 and 2 have significantly higher quantum efficiencies, which will raise the overall system efficiency to up to 35–40%. The first 'RG' detector has now arrived at the test lab and features a quantum efficiency of 0.87 and 0.82 at 1 and 2μm, a read noise of 3.1e−, and a dark current <0.01e−/s/pixel.

The new detectors require a change in design of the detector stage, which is presently being built. Also, the read-out electronics will be updated. We do not use the Hawaii-2 RG "SIDECAR" ASIC but use the read-out electronics developed by the MPIA detector group.

The complete package is presently being cold-tested and characterized in Germany in the lab and will be integrated into LUCI-2 in July 2012.

5.2 Active flexure compensation

With the new 'RG' detector and the possibility to define regions of interests that can be read-out separately having different exposure times it becomes feasible to use a small part of the detector for image motion tracking. This could be used to upgrade the flexure compensation to an active mode instead of the present lookup-table approach.

5.3 Binocular operations

From 2013 on both LUCI instruments will be mounted at the telescope. This provides an immense boost in efficiency - essentially doubling the observation capabilities in the near-infrared- and in versatility. As stated above, the maximum angular separation of the two instrument's FOVs on sky is 40". This is due to the binocular mount design of the LBT where the placement of the FOVs is limited by the working range of the active optics system. The design of the instrument control allows both instruments to be used together or independently, in imaging or spectroscopy – each one with or without adaptive optics. It will also be possible to apply different dither schemes to both LUCI instruments by using the active optics of the telescope (within maximum separation field given above).

5.4 Natural guide star AO, wide-field AO, Ground Layer Adaptive Optics

AO System

The adaptive optics correction is realized through an adaptive secondary mirror. Therefore all instruments on the Cassegrain and Bent-Gregorian focal stations can benefit from the facility AO system. 672 electro-magnetic force actuators manipulate the shape of the adaptive secondary mirror shell that has a diameter of 0.91m while it is only 1.5mm thick. Wavefront sensing, reconstruction and corrections are carried out at a rate of 1kHz (Esposito et al. 2003 [3]). As an upgrade, the ground layer adaptive optics (GLAO) facility 'ARGOS' (Rabien et al 2010 [5]) is currently built at MPE and various partner institutes. ARGOS utilizes three pulsed lasers per primary mirror to project multiple Rayleigh laser guide stars onto the sky for homogeneous field correction. The green 532nm lasers, pulsed at 10 kHz, are focussed to an altitude of around 12km in the atmosphere. The returning scattered photons are electro-optically range-gated to ±150m around the focussing altitude before entering the wavefront sensing unit. A separate tip-tilt sensing unit provides the necessary correction of the tilt introduced by the atmosphere, taking the light from an additional natural tip-tilt star. The correction of the science light wavefront does not fully achieve the diffraction limit. It rather yields a decrease of the PSF FWHM and an increase of the encircled energy by a factor 2-3 over the full field of view of 4′×4′. This yield corresponds to a gain of a factor 4-9 in integration time.

LUCIs AO camera and AO use

Diffraction-limited imaging and high-resolution will be provided by the "N30" camera, which features a cassegrain design. The cameras are currently being cold-tested in the lab. LUCI-2 will have the AO system built-in once it is shipped to the mountain. LUCI-1 will be upgraded thereafter.

The usable FOV for diffraction-limited imaging is 30x30arcsec^2 and a slit width of around 0.1 arcsec would result in a high spectral slit-limited resolution of ~10.000.

In AO mode, the H+K grating becomes usable as an H *or* K grating at R~4000 (slit limited resolution) using the (non-AO) N3.75 camera and a quarter arcsecond slit. MOS spectroscopy on the full FOV will benefit immensely from this observing mode which will be afforded by the ARGOS system.

MCAO

In a further step, ARGOS can be upgraded with an additional 589nm sodium laser guide star to achieve diffraction limited observations in a multi-conjugated adaptive optics setup. Since the wavefront is already pre-corrected by the GLAO, resulting in a increase in r_0, less laser power is needed which greatly facilitates this possible upgrade [5]).

5.5 Spherically curved MOS masks

Currently the MOS masks only correct for the curvature of the focal plane in one direction, i.e. they follow a cylindrical shape. Presently no science has suffered from the small defocus of slits near the edge of the FOV (in dispersion direction), especially since slits near the edge produce spectra that extend significantly beyond the detector area and are therefore seldom placed in these areas. With the advent of the ARGOS wide-field AO, it is desirable to have the mask's curvature follow the focal plane in both directions. We presently investigate on the manufacturing of the mask blanks.

5.6 Additional Observing modes

The current space envelope used inside the cryostat allows for additional hardware with access to the focal pane and the entrance beam. This space could be used to extend the instrument observation modes in the future, e.g. to provide integral-field observations or OH line filtering in imaging and spectroscopy.

REFERENCES

[1] Ageorges, N., Seifert, W., Jütte, M., et al., "LUCIFER1 commissioning at the LBT", Proc. SPIE 7735, 77351L-77351L-12 (2010)

[2] Buschkamp, P., Hofmann, R., Gemperlein, H., Polsterer, et al., "The LUCIFER MOS: a full cryogenic mask handling unit for a near-infrared multi-object spectrograph", Proc. SPIE 7735, 773579-773579-12 (2010)

[3] Esposito, S., Tozzi, A., Puglisi, A., et al., "Development of the first-light AO system for the large binocular telescope", Proc. SPIE 5169, 149-158 (2003)

[4] Polsterer, K., Jütte, M., Knierim, V., et al., "Lucifer VR: a virtual instrument for the LBT", Proc. SPIE 6274, 62740M (2006)

[5] Rabien, S., et al., "ARGOS: the laser guide star system for the LBT", Proc SPIE 7736, 77360E-77360E-12 (2010)

[6] Seifert, W., Appenzeller, I., et al., "LUCIFER: a Multi-Mode NIR Instrument for the LBT", Proc. SPIE 4841, 962-973 (2003)

[7] Seifert, W., Ageorges, N., et al., "LUCIFER1: Performance results", Proc. SPIE 7735, 77357W-77357W-9 (2010)